SCA-9826

CORRELATION OF ROCK PERMEABILITY AND ANISOTROPIC STRESS CONDITIONS FOR THE INTEGRATION OF ROCK MECHANICAL AND HYDRAULIC FLOW MODELS

G. Pusch* and J. R. Weber**

Abstract

The transfer rules of hydraulic rock parameters from laboratory to in-situ conditions are mainly basedon isotropic, elastic rock deformation principles. However the stress field in the neighborhood of underground cavities, like shafts, tunnels, wells etc is not isotropic. Biaxial stress conditions have been realized in experiments to investigate the relationship between rock permeability and axial and radial stress. From deep drilling projects, gneiss rock samples, a metamorphic sedimentary rock and Rotliegendes sandstone samples from an outcrop have been investigated in compression tests to correlate permeability change and deviatoric stress magnitude. For both rock type samples a characteristic ratio between axial and radial stress could be determined where permeability reaches a minimum value. A further increase of the deviatoric stress magnitude increases permeability by pore volume dilatancy, the formation or reopening of microfractures. A mathematical correlation has been developed to describe the characteristic permeability performance with varying radial and axial stresses. This correlation is capable to define the critical boundary of rock dislocation by shear-stress and to couple hydraulic and mechanical models.

1. Introduction

The conversion of rock properties like porosity and permeability to downhole or in situ-conditions is routinely based on compressive stress-strain relationships. In a stress field, which is free from sinks and sources, isostatic stress conditions can be assumed in underground porous formations. This situation however changes in the vicinity of shafts, wells, storage caverns, tunnels and underground galeries, where the tangential and radial stress are different at the wall of the cavity. As a consequence the deformation of the rock leads to embrittlement, microfracturing, fracture and disintegration of rock zones and transportation of rock fragments (sand production). The whole spectrum of phenomena from dislocation to fracturing is controlled by the continuum-mechanics principle. For a variety of materials – unconsolidated and consolidated sands, crystalline rocks, clay, rock salt etc. – the stress-strain relationship is well defined from elastic to viscous behavior, comprising all intermediate stages of elastoplastic to viscoplastic state. The most complicated material behavior of salt rocks even includes time dependent effects, like creeping, which has to be taken into account in rock mechanical models.

The deformation of porous media is mathematically characterized by the superposition of elastic and non-elastic strain components. If the deviatoric stress ratio, that is the ratio of the maximum and the minimum normal stress is low, the compression-state of pore space deformation dominates. If a critical stress ratio is exceeded, the increasing shear

* TU Clausthal
** BGR, Hannover

tension leads to an extension of the pore volume (dilatancy). The mathematical algorithms for the correlation of stress – strain – permeability relations are based on power law functions and the cubic root law for the permeability of fissure-networks. Walsh and Witherspoon (19,22) have described such functions for crystalline rocks, Wagner (18), Ali (1), Jones (6) and Wilhelmi (21) for sedimentary rocks. An example is shown in Figure 1.

For increasing deviatoric stress ratios, Holt (4) describes a pronounced permeability reduction for North Sea reservoir rocks (sandstones), if the elastic deformation boundary of roughly 70 MPa is exceeded. This may lead to plastic deformation of the near wellbore zone and to sand production. In compression experiments with Dalquhandy-sandstone Smart (14) observes a permeability and corresponding strain minimum, which leads to disintegration of the rock. Zoback (23) has performed experiments with Westerly-granite and correlates a pore volume and permeability dilatancy with the deviator stress after exceeding the critical stress ratio σ_1 / σ_3, as it is shown in Figure 2.

Similar phenomena are reported for subbituminous coal by Hoffmann (3) and for rock salt by Borgmeier (2). Coupled mechanical and hydraulic material laws are rare in the literature. Most algorithms describing this phenomena are based on a nonlinear relationship between permeability and pore volume of a simplified capillary flow model, as for example Stormont (16) for rock salt. Recently numerical simulation programs have been described in the literature and have been applied for reservoir studies, which take into account the coupling of mechanical and hydraulic properties of the rock (7,17).

In this paper, rock triaxial-permeability experiments and mathematical algorithms are described, which correlate normal stress and permeability. The shape of the permeability -dilatancy curve is used to derive the boundary for the initiation of microfracturing and the material and stress specific Poisson ratio.

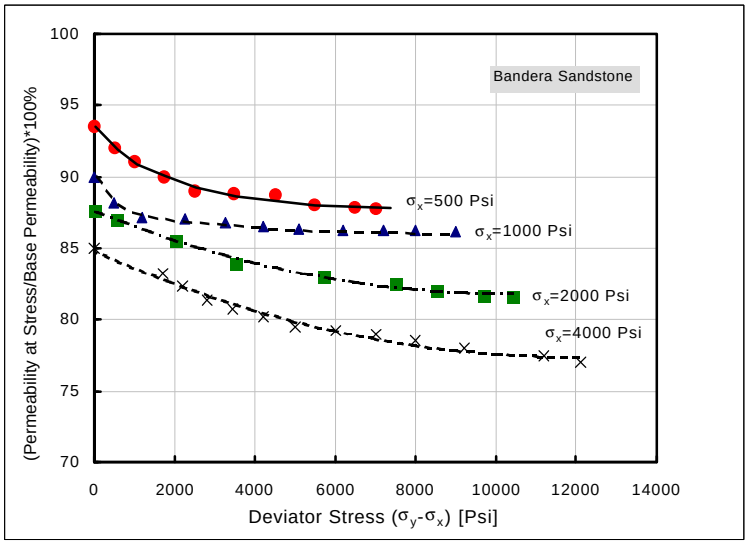

Fig. 1: Permeability Change of Bandera Sandstone under Stress Conditions after Wilhelmi et al. (21).

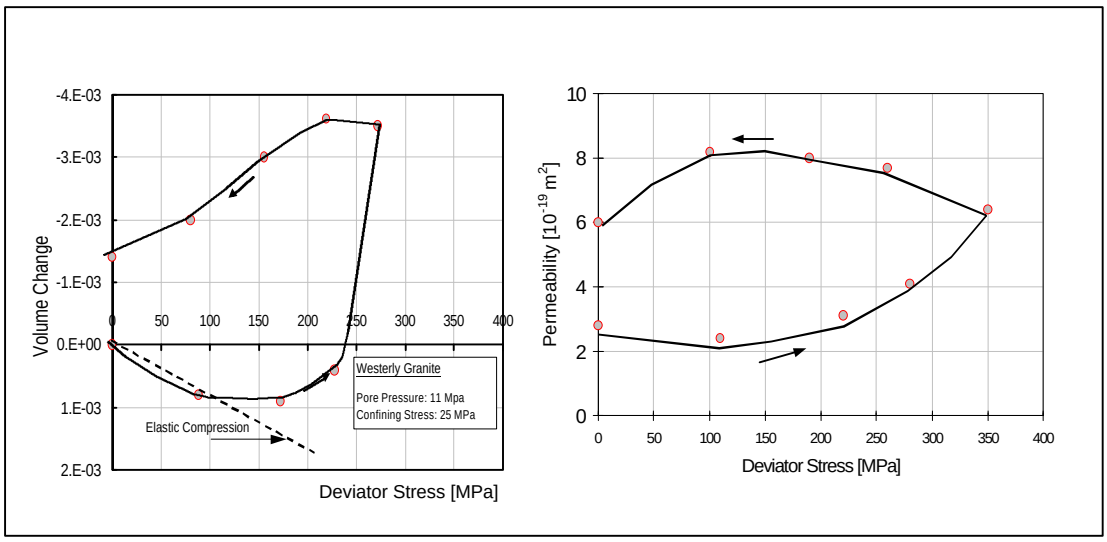

Fig 2: Volume and Permeability Dilatancy of Westerly Granite after Zoback et al. (23)

2. Experimental

A triaxial cell and hydraulic loading system, capable of stresses up to 230 MPa and a maximum temperature of 200 °C, which contains a coreholder with a viton sleeve was used for the experiments. The pressure loading rates were carefully adjusted to the material strength and deformation relaxation time. The pore pressure for the gaseous phase nitrogen, which was used as a hydraulic fluid in the percolation experiments, was limited to a maximum of 1 MPa. For a general classification of the rock permeability the slippage effect of the gas was corrected after Klinkenberg. In the compression test cyclic loading experiments, the Klinkenberg correction was not used. However the pore pressure was kept near the maximum value of 1 MPa in order to minimize the influence of the slipping effect on the measured permeability. All experiments described in this report have been performed at ambient temperature of 20 °C. The rock properties of samples tested in the laboratory, are described in Table 1.

The rock components investigated are from the class of low permeable porous media, as for example Rotliegendes sandstone, metagneis, rock salt and hard coal. In the few lab tests, which are shown in this paper, the orientation of the core axis was determined with respect to foliation, layering and to the axis of the underground cavity. The material properties of the individual rocks have been measured independently by geomechanical standard tests or are derived, as indicated, from the literature.

Figure 3 shows the result of a cyclic loading and unloading compression-experiment, using a very tight crystalline rock sample from the deep drilling project in Germany (KTB-Well). The mineralogic composition defines this rock as a metagneiss, which was drilled parallel to the foliation of the rock. In 3 loading cycles the permeability level of the sample is increased from 2.2 nD up to 4.5 nD without disintegration. The permeability

minima of the three loading curves are progressively displaced to a lower dilatancy boundary. This typical behavior was observed in many experiments, characterizing a so called ‚rock softening' phenomenon when the maximum stress is parallel to the foliation direction and tensile forces at the peak of existing micro-inhomogeneities (Griffith Cracks) activate the generation of new flow paths.

Table 1: Sample Characterization

No	Rock Type, Geologic Age	Origin	Orientation	Dimension L×D, cm	Porosity f, %	Permeability m^2	Material Properties Young Modulus, GPa	Poisson Ratio
1	Sandstone (Rotliegendes)	Outcrop [15] Flechtinger Bausandstein	Perpendicular to Layering	10 × 5	10.5	8×10^{-16}	11.9 (± 20 %)[15]	0.23 – 0.33 [10] at normal stress of 14–56 MPa .
2	Gneiss (Paleozoic)	KTB – deep[20] drilling project (349 C1 mE)	Parallel to Foliation	3.2 × 3	1.5	3.3×10^{-17}	27.4 (± 50 %)[12]	0.08 – 0.14 [11] at normal stress of 1 – 6 MPa.
3	Rock Salt (Zechstein)	Gas Storage[2] (Core No 23)	Perpendicular to Cavern Axis	10 × 6	0.5	1×10^{-16}	19 -42 [24]	0.33 – 0.36 [11] (from seismic) 0.1 –0.25 [11] (from lab tests)
4	Subbituminous Coal (Westphalian)	Coal Mine[3] Warndt, Seam No 5 (Core 29.4)	Parallel to Layering	9 × 6	7.5	2.4×10^{-16}	3.4 – 7.0 [3]	0.1 – 0.3 [13] (degassed coal) 0.25 – 0.5[11] (British Coal Mines)

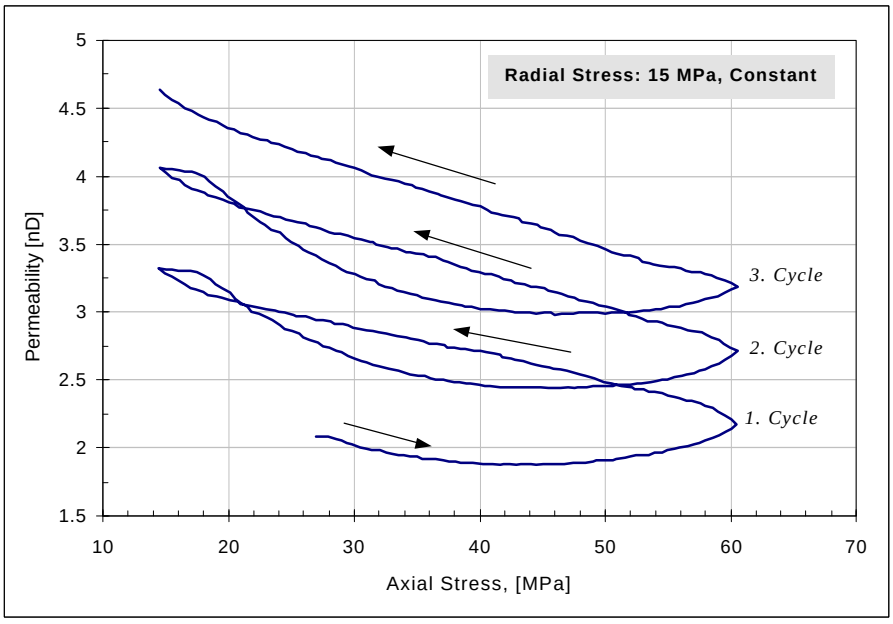

Fig. 3: Cyclic Loading-Compression Experiment with a Metagneiss Sample from the Deep-Drilling Project in Germany- Strain Softening.

In the following Figure 4 the stress loading cycles show the opposite material behavior. The permeability level is reduced in the second loading cycle and the permeability minimum displaced to a higher critical dilatancy boundary. This behavior was called “stress hardening” phenomenon. In contrast to the sample of Figure 3 this core from the KTB-Well, characterized as Gneiss, was drilled perpendicular to the foliation. The hypothetical explanation for the stress hardening is based on a parallel shift of the existing micro-fracture plains. Induced by the surface smoothing, the fracture width and thereby the microfracture permeability is reduced. In Figure 5 the results of a deviatoric compression test with a sample from Rotliegendes Sandstone is represented. It was determined by T. Stammnitz (15), using the same experimental method and set-up. It is apparent from the shape of the curve, that the permeability increase is more pronounced than for the crystalline rock sample. Strain hardening and softening could not be detected, since only the stress build up phase was recorded.

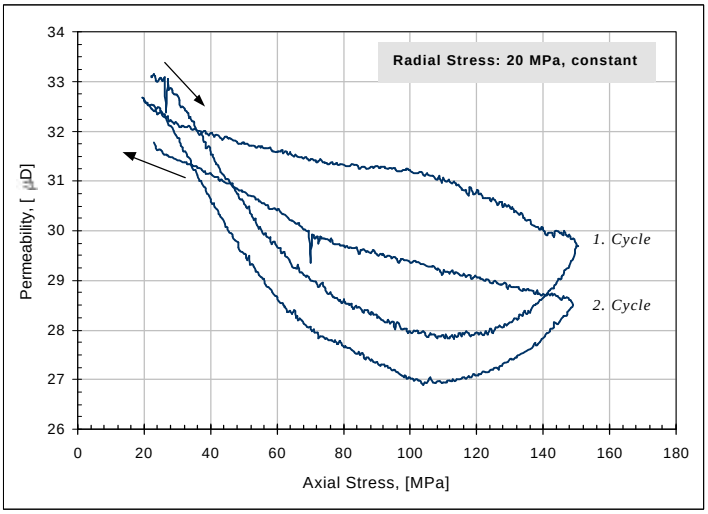

Fig. 4: Cyclic Compression Experiment with a Gneiss Sample from the Deep-Drilling Project in Germany-Strain Hardening.

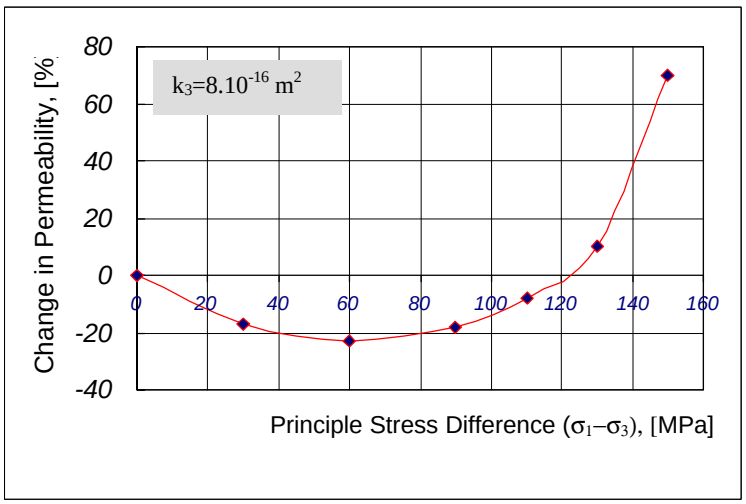

Fig. 5: Compression Test with a Rotliegendes Sandstone Sample –Permeability Dilatancy

3. Mathematical Algorithm for the Correlation of Normal Stress and Permeability

For a true physical characterization of the stress field and the hydraulic properties of the rock, stress parameters and permeability must be handled as tensors. In most cases this complicated system can be reduced to a 2-dimensional representation into vertical and horizontal stress as well as for permeabilities parallel and perpendicular to the layer. This simplified approach will be used in characterizing the relationship between stress and permeability in our model. However, the structure of the algorithm is indifferent for the 2 components. For the modeling of the compressional deformation the power law function as described by Ali (1) or by Kranz (8) will be used. The superposition of the growing influence of shear stress with the magnitude of the deviator σ_1/σ_3 will be represented by an exponential function as shown in Formula 1.

$$\frac{k_1}{k_3} = \left(a \frac{s_1}{s_3} \right)^{-n} \exp\left[A\left\{ \left(\frac{s_1}{s_3} \right)^{m} - 1 \right\} \right] \tag{1}$$

where:

k = permeability
σ = normal stress
A = coefficient
a = scale factor

and super and subscripts,
m,n = exponents
1 = maximal stress
3 = minimal stress

The index 3 refers in this algorithm to the minimal normal stress, which is for a compressional test the radial stress. Therefore the corresponding permeability is taken as the initial value for isostatic conditions where σ_1 equals σ_3. The index 1 refers to the maximal normal stress, which is for a compressional test the axial stress. The algorithm contains 4 adjustment parameters. The parameters n and m characterize the dip of the compressional and dilatancy branch of the curve. The parameter A is responsible for the position of the minimum with respect to the x-axis. The parameter a is a scale factor and shifts the curve with respect to the y-axis. Figure 6 shows the sensitivity of the shape of the curve with respect to these 4 parameters. The permeability minimum of Equation 1 can be derived for the following stress ratio σ_1/σ_3

$$\left(\frac{s_1}{s_3} \right) = \sqrt[m]{\frac{n}{A.m}} \tag{2}$$

The minimum defines the lower boundary of dilatancy effects and can be correlated with the material property of an instantaneous Poisson ratio. For the derivation isotropic material properties with respect to the radial distribution in a core must be assumed.

Assumption : Pore pressure is negligible; isotropic material properties

$$e_3 = \frac{1}{E}\left[s_3 - n\left(s_3 + s_1 \right) \right] \tag{3}$$

Since the core holder eliminates radial expansion of the core,

$$e_3 \cong 0$$

and the radial stress field is homogeneous

$$s_3 = n(s_3 + s_1)$$

and dividing the above Equation by s_3

$$n_{crit} = \left(\frac{s_1}{s_3} + 1 \right)^{-1} \tag{4}$$

The permeability minimum, which defines the beginning of dilatancy effects should therefore correspond to a critical Poisson ratio as determined by Equation 4. This correlation has been applied to the experimental results of compressional tests, with permeability dilatancy for different rock materials.

4. Modeling Results

Individual experiments with representatives of sandstone rock, crystalline rock, salt rock and hard coal have been matched with the algorithm of Equation 1, as it is shown in Fig. 7– 10.

The measured permeability data were normalized with respect to the initial isostatic stress conditions, that is equal axial and radial stress, represented by term k_3 in Eq. 1.

The regression quality for all 4 matches is better than 94 %. The correlation of the calculated minima with the critical Poisson ratio is in a good agreement with the material properties measured independently for the same rock type or derived from literature as indicated in Table 2.

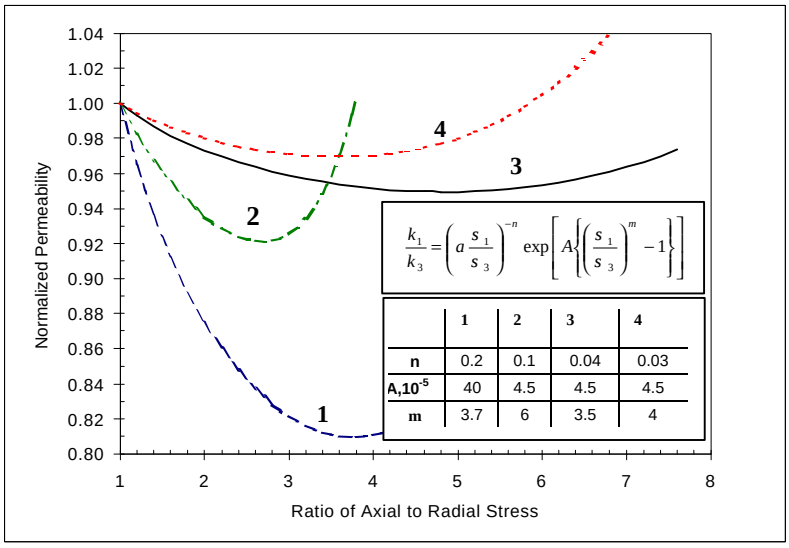

	1	2	3	4
n	0.2	0.1	0.04	0.03
A,10^{-5}	40	4.5	4.5	4.5
m	3.7	6	3.5	4

Fig. 6: Parametric Study of the Stress –Permeability Correlation Function.

This critical Poisson ratio defines the transition between elastic and plastic rock deformation and can therefore be used to estimate the deviatoric stress conditions, where microfracturing begins. However it is not possible to estimate the upper boundary of infinite permeability, where disintegration of the rock begins without an extension to a rock mechanical fracture law.

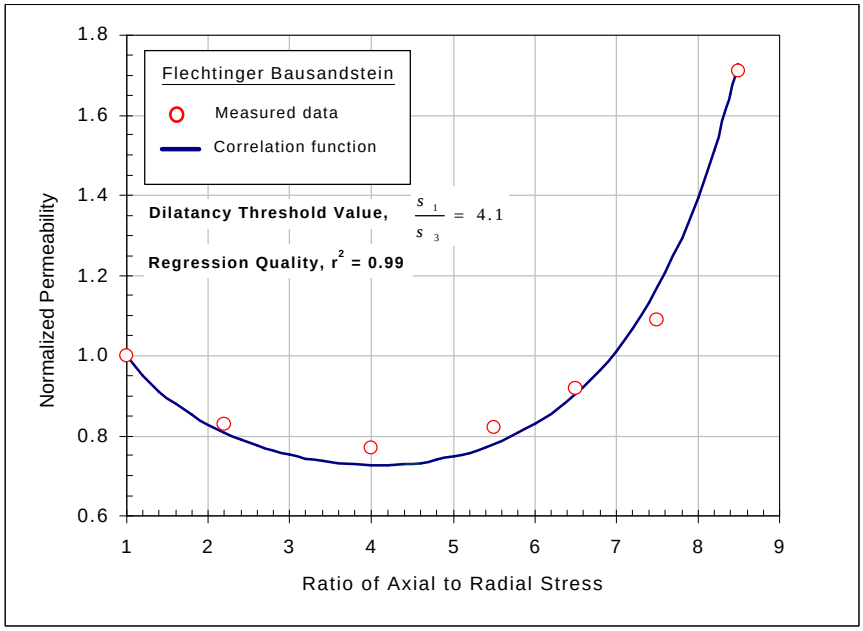

Fig. 7: Correlation of Measured Compressional Test Data by the Use of the Formula 1 – Flechtinger Bausandstein.

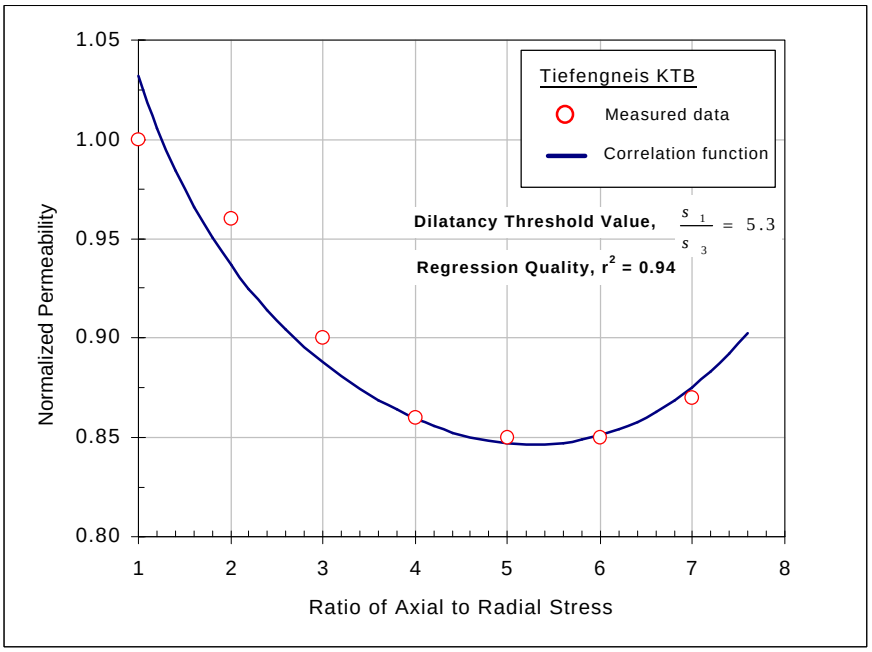

Fig. 8: Correlation of Measured Compressional Test Data by the Use of the Formula 1- Tiefengneis KTB.

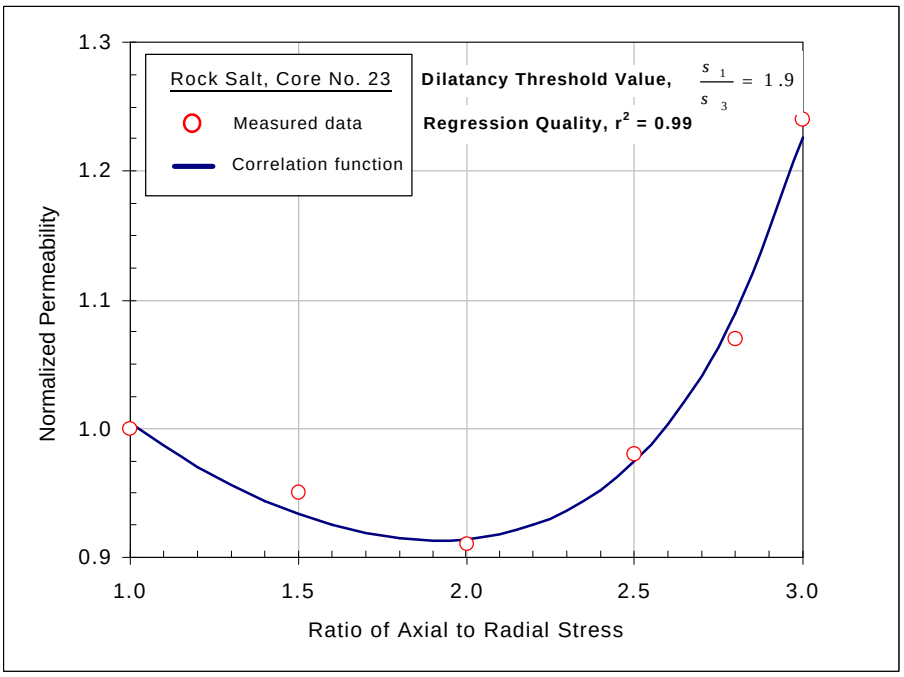

Fig. 9: Correlation of Measured Compressional Test Data by the Use of the Formula 1 – Rock Salt.

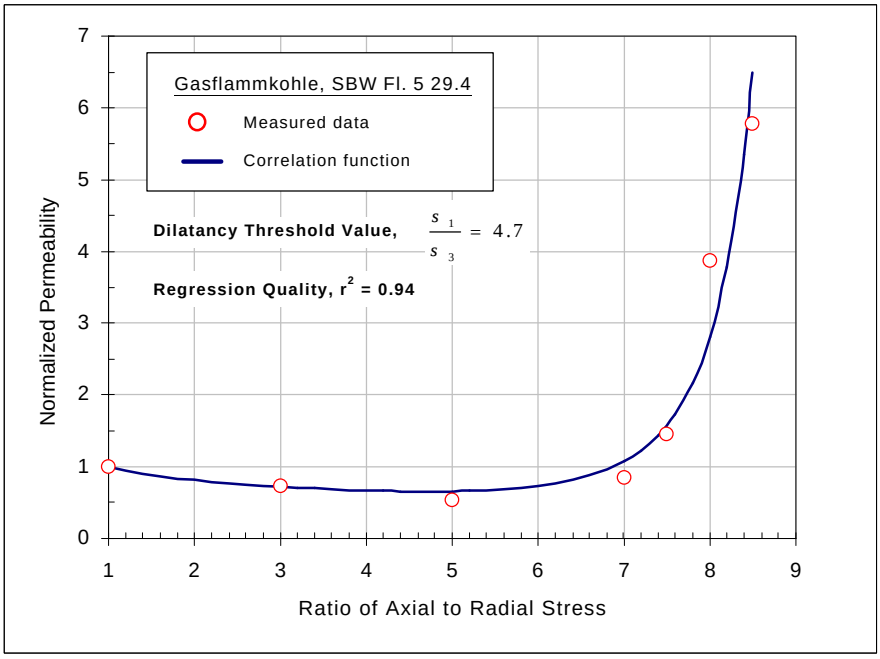

Fig. 10: Correlation of Measured Compressional Test Data by the Use of the Formula 1 – Subbituminous Coal.

Table 2 : Results of Matching Procedure

Rock Type	*Permeability Range, mD*	*Orientation*	*Critical Stress Ratio*	*Poisson Coefficient*	
				Derived	*Measured*[*]
Sandstone[15] (Rotliegendes)	0.80	Perpendicular to Layering	4.08	0.20	0.21 [15]
Gneiss [20]	0.03	Parallel to Foliation	5.28	0.16	0.15 [12]
Rock Salt [2]	0.10	Perpendicular to Cavern Axis	1.92	0.34	0.33- 0.36[11]
Degassed Subbituminous Coal [3]	0.24	Parallel to Layering	4.70	0.175	0.10- 0.30[13]

[*] Triaxial Strain Test, Seismic Measurement

5. Conclusions

Triaxial compressional tests have been performed to determine the permeability-dilatancy of different rocks. It became obvious that this phenomenon can be interpreted as the reopening of existing micropores/microfracs or the generation of new flow paths accompanying the dislocation of a rock under a deviatoric stress regime. An empirical correlation was shown which is able to match the experimental results satisfactorily and to determine the permeability minimum as an indicator for the beginning of pore volume dilatancy.

The critical stress ratio at this minimum can be converted into a critical Poisson-coefficient ν, which fits quite well to independent measurements of ν under the regime of elasto-plastic stress-strain behavior. Further investigations are necessary to correlate the empirical parameters with physical stress-strain models.

References

1. Ali, H. S. et al., The Effect of Overburden Pressure, SPE-Paper 15730 5. SPE Middle-East Oil Show Proc., Manama, Bahrain, March 1987, 7-10.

2. Borgmeier, M., Untersuchungen zum belastungsabhängigen Durchlässigkeitsverhalten von Salzgestein für Gase unter besonderer Berücksichtigung der Porenraumbeladungen, Dissertation 1995, TU Clausthal.

3. Hoffmann, M., Einfluß der Gasadsorption und des Spannungszustandes auf die Poren-raumeigenschaften der Steinkohle, Dissertation 1988, TU Clausthal.

4. Holt, R.M., Permeability Reduction Induced Nonhydrostatic Stress Field, SPE-Paper 19595 Annual Techn. Conf., San Antonio, Oct. 8-11, 1989.

5. Hou, Z., Untersuchungen zum Nachweis der Standsicherheit für Untertagedeponien im Salzgebirge, Dissertation 1997, TU Clausthal.

6. Jones, F.O., A Laboratory Study of the Effects of Confining Pressure on Fracture Flow and Storage Capacity in Carbonate Rocks, *Journal of Petr. Tech*. 1 (1975), 21 – 27.

7. Koutsabeloulis, N.C., Coupled Stress/Fluid/Thermal Multiphase Reservoir Simulation Studies Incorporating Rock Mechanics SPE-Paper 47393 EU ROCK 98,Trondheim, July 8-10, 1998.

8. Kranz, R.L. et al., The Permeability of Whole and Jointed Barre Granit, Int. Journal of Rock Mech., Min.Sc. and Geomechanics, 16, (1979), 225-234.

9. Van Krevelen, D.W., *Coal, Typology - Chemistry- Physics- Constitution*, Amsterdam Oxford-New York, 1981.

10. Link, H., *Zur Querdehnungszahl des Gebirges, Geologie und Bauwesen* 26, 1961, 246-257.

11. Link, H., *Zur Querdehnungszahl von Gestein und Gebirge, Geologie und Bauwesen* 27 1962, 89-100.

12. Natau, O., Roechel, T., Rock Mechanics, KTB Report 95-2, 1995, Hannover.

13. Phillips, D.W., Rock Bursts or “Bumps” in Coal Mines, Transact. Inst. Mining Eng., 104, 1954/55, 55.

14. Smart, B.G. et al., The Effects of Combined Changes in Pore Fluid Chemistry and Stress State on Reservoir Permeability, PSTI-Technical Bulletin No. 1, 1992, 14-17.

15. Stammnitz, Th., Entwicklung einer Methode zur Untersuchung der Belastungsabhängigkeit von Porosität und Permeabilität sowie deren Beziehung zur Gesteinsdeformation, Dissertation 1992, TU Clauthal.

16. Stormont, J.C. et al., Predictions of Dilatation and Permeability Changes in Rock Salt, *Int. J. for Numerical and Analytical Methods in Geomechanics*, 16 (1992), 545-569.

17. Teufel, L.W. et al., A Two-Domain,3-D Fully Coupled Fluid-Flow/Geomechanical Simulation Model for Reservoirs with Stress–Sensitive Mechanical and Fluid-Flow Properties SPE-Paper 47397, EU ROCK 98, Trondheim, July 8-10,1998.

18. Wagner, C., Vogt, M., Eine Methode zur Bestimmmung der Porosität und Kompressibilität Poröser Gesteine unter Gebirgsdruck, Zt. für Angewandte *Geologie* 17, (1971), 10, 413 – 416.

19. Walsh, J.B., Effect of Pore Pressure and Confining Pressure on Fracture Permeability, *Int. Journal of Rock Mech. Min.Sc. and Geomechanics* 18, (1981), 429-435.

20. Weber, J. R., Untersuchungen zur Permeabilitätsdilatanz kristalliner Gesteine unter deviatorischer Belastung, Dissertation 1994, TU Clausthal.

21. Wilhelmi, B., Somerton, W.H., Simultaneous Measurement of Pore and Elastic Properties of Rocks under Triaxial Stress Conditions, *SPE-Journal*, (1967), 9, 283 – 294.

22. Witherspoon, P.A., Validity of the Cubic Law for Fluid Flow in a Deformable Rock Fracture, *Water Resources Res*. 16, (1980), 6, 1016-1024.

23. Zoback, M.D., Byerlee, J.D., The Effect of Microcrack Dilatancy on the Permeability of Westerly Granite, *Journal of Geophys*. Res. 80, (1975), 752-755

24. Hardy, H.R. and Langer, M., The Mechanical Behavior of Salt, Trans. Tech. Publ., (1984), Clausthal.